energies

MDPI

Article

Numerical Study on the Homogeneous Reactions of Mercury in a 600 MW Coal-Fired Utility Boiler

Qiang Lyu [1], Chang'an Wang [1,*], Xuan Liu [2,3] and Defu Che [1]

[1] State Key Laboratory of Multiphase Flow in Power Engineering, School of Energy and Power Engineering, Xi'an Jiaotong University, Xi'an 710049, China; qianglv@xjtu.edu.cn (Q.L.); dfche@mail.xjtu.edu.cn (D.C.)
[2] College of Environmental Science and Engineering, Hunan University, Changsha 410082, China; liuxuanne@hnu.edu.cn
[3] Key Laboratory of Environmental Biology and Pollution Control, Hunan University, Ministry of Education, Changsha 410082, China
* Correspondence: changanwang@mail.xjtu.edu.cn

Abstract: The homogeneous oxidation of elemental mercury (Hg^0) can promote Hg pollution control in coal-fired power plants, while the mechanisms and quantitative contributions of homogeneous reactions in Hg^0 oxidation, especially the reactions between Hg and chlorine (Cl), are still unclear. Here, a numerical study on the homogeneous reactions of Hg was conducted within a 600 MW tangentially fired boiler for the first time. A novel Hg sub-model was established by coupling the thermodynamics, reaction kinetics and fluid dynamics. The results showed that the higher Cl content in coal was beneficial to the oxidation of Hg^0. The homogeneous reactions of Hg mainly occurred in the vertical flue pass at low temperature. Hg^0 was still the dominant Hg-containing species at the boiler exit, and the concentration of mercury chloride ($HgCl_2$) was the highest among the oxidized mercury. When low-Cl coal was fired, the addition of a small amount of chlorine species into the boiler at the burnout area increased the ratio of $HgCl_2$ by over 16 times without causing serious chlorine corrosion problems.

Keywords: mercury; computation fluid dynamics (CFD); homogeneous reaction; utility boiler; chlorine

check for updates

Citation: Lyu, Q.; Wang, C.; Liu, X.; Che, D. Numerical Study on the Homogeneous Reactions of Mercury in a 600 MW Coal-Fired Utility Boiler. *Energies* **2022**, *15*, 446. https://doi.org/10.3390/en15020446

Academic Editor: Giancarlo Sorrentino

Received: 6 December 2021
Accepted: 7 January 2022
Published: 9 January 2022

1. Introduction

Coal-fired utility boilers are the predominant anthropogenic mercury (Hg) sources in many regions around the world [1,2]. Mercury is released from coal during the combustion process, with only about 2% of mercury remaining in the bottom slag. Mercury in flue gas mainly exists in three forms: gaseous elemental mercury (Hg^0), gaseous oxidized mercury (Hg^{2+}) and particulate mercury (Hg_p) [3–5]. Among them, gaseous oxidized mercury has high solubility and can be removed in wet flue gas desulfurization devices. Particulate mercury can be collected using particulate matter control devices, such as electrostatic precipitators (ESPs) and fabric filters (FFs). As a result, most mercury emitted to the atmosphere from coal-fired power plants is in the form of gaseous elemental mercury, which is difficult to remove. Gaseous elemental mercury is the only stable form of mercury in the temperature range of furnaces (1050~1400 °C). During the combustion process, the flue gas temperature decreases gradually as the flue gas flows. Part of Hg^0 will then be oxidized into Hg^{2+} by other flue gas components, while some of the Hg^0 will be captured by fly ash particles [6]. Some scholars have carried out thermodynamic equilibrium analyses on mercury species and have reported that only Hg^0 can exist stably when the temperature is higher than 750 °C, while all Hg^0 will be oxidized into Hg^{2+} if the temperature is below 450 °C [7,8]. However, the measured data show that Hg^0 still occupies a large proportion of Hg emitted from the flue gas because the oxidation process of Hg^0 is limited by the kinetic factors [9,10]. For example, Chen et al. reported that the fractions of gaseous elemental mercury, gaseous oxidized mercury and particulate

mercury before ESP/FF are 10.4%~93.2%, 3.7%~44.3% and 1.3%~59.5%, respectively [9]. The migration of mercury species in coal-fired boilers is affected by the coal type and boiler operating conditions [7,11–13]. Additionally, the concentrations of HCl, NO_x, SO_2 and other components in flue gas also greatly influence the oxidation reactions of Hg^0 [12,14].

The oxidation processes of Hg^0 in flue gas include homogeneous oxidation and heterogeneous oxidation. Homogeneous oxidation refers to the redox reactions between Hg^0 and flue gas components within the boiler. Heterogeneous oxidation occurs on the surfaces of adsorbents or catalysts, for which the reaction temperature is even lower. The influence of HCl on the homogeneous oxidation of Hg^0 was studied by Sliger et al. [15]. The results showed that increasing the concentration of HCl could increase the temperature zone of homogeneous Hg reactions significantly, which meant that Hg^0 could be oxidized earlier in the boiler. Galbreath et al. conducted a bench-scale study on a 7 kW coal combustion system and found that the HCl addition could enhance the oxidation of Hg^0 significantly [16]. Wang et al. focused on the heterogeneous oxidation of Hg^0 and compared the influences of NaCl, $CaCl_2$ and HCl additions [17]. However, compared with the extensive investigations on heterogeneous mercury reactions, the research on the homogeneous reactions of mercury in a full-scale utility boiler is still insufficient [18,19]. The distributions of the mercury-related species inside the furnace and flue pass are yet to be revealed. Considering the decisive role of the forms of mercury species in choosing the mercury removal approach, it is necessary to investigate the homogeneous reactions between mercury and other flue gas components for mercury emission control from coal-fired power plants.

Because of the extremely low concentrations of Hg and its compounds, it is difficult to carry out experimental studies on the homogeneous reaction of mercury. The computational fluid dynamics (CFD) method is an alternative way to investigate the homogeneous reactions of Hg in coal-fired utility boilers. Taking into account the vital influences of Hg-Cl reactions on the homogeneous oxidation of Hg^0, we conducted this numerical study with the following aims: (1) revealing the influence of the chlorine content in coal on the homogeneous reactions of Hg; (2) evaluating the quantitative impacts of the addition of Cl-containing species on the homogeneous oxidation of Hg^0 inside a full-scale boiler.

For the first time, a novel mercury sub-model was established in a full-scale tangentially coal-fired boiler to achieve the coupling of thermodynamics, reaction kinetics and fluid dynamics. The thermodynamics data for mercury species and the kinetics data for the elemental reactions are needed to conduct the simulation of the homogeneous mercury reactions. In addition to the homogeneous reactions of Hg, the flow field, the temperature field and the flue gas component distribution within the boiler were also analyzed. The results of this work are of significance in understanding the mechanisms of homogeneous Hg reactions and will lay a foundation for efficient mercury pollution control in coal-fired utility boilers.

2. Utility Boiler and Input Parameters

2.1. Boiler Description and Mesh Generation

Supercritical tangentially boilers are widely used in coal-fired power plants because of their good flame fullness and high combustion efficiency [20–23]. Therefore, a 600 MW supercritical tangentially fired boiler was chosen in this study, as shown in Figure 1a. The width, depth and elevation of the furnace of this boiler were 18,816 mm, 17,696 mm and 72,350 mm, respectively. The geometric model of the solution area was built using SOLIDWORKS according to the structure of the boiler. Appropriate simplifications were employed during the model construction. For example, the thicknesses of the water wall and the heat exchanger was considered as zero. Each corner of the furnace was equipped with 6 layers of primary air (PA) nozzles, including one layer for standby. Additionally, the specific layouts of auxiliary air (AUX) nozzles, close-coupled over fire air (CCOFA) nozzles, underfire air (UFA) nozzles and separated over fire air (SOFA) nozzles are shown in Figure 1b.

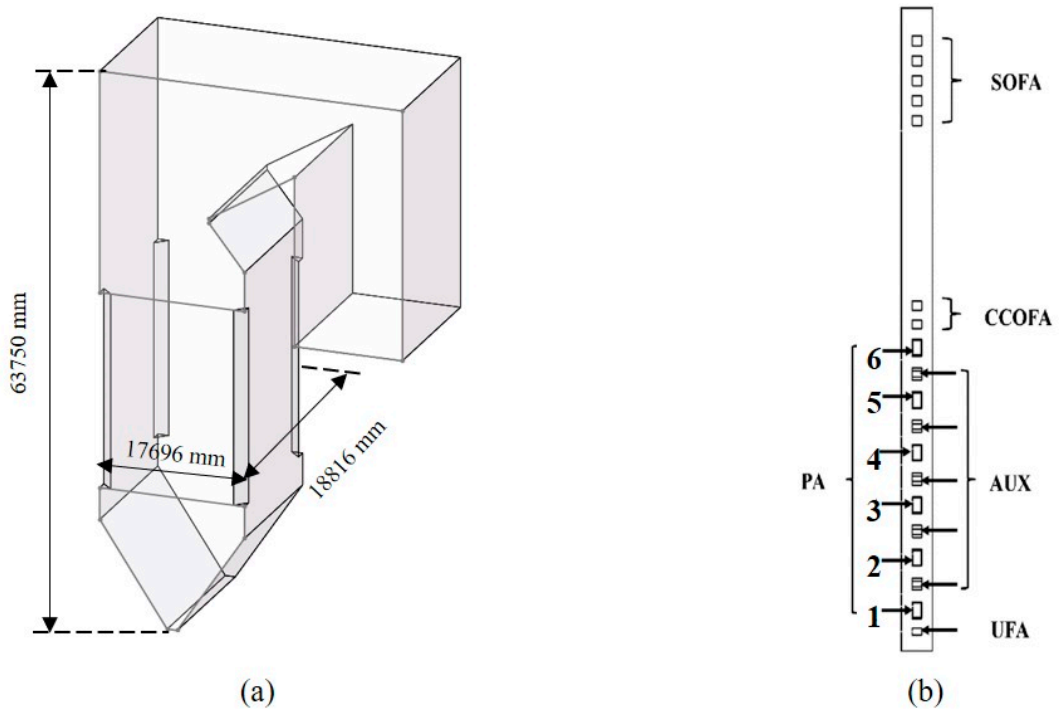

Figure 1. Structure of the boiler and arrangement of the nozzles: (**a**) utility boiler; (**b**) nozzle arrangement.

ICEM software was used to generate the hexahedral structured mesh system of the boiler. The mesh near the burner area was refined to improve the accuracy of the simulation results. Three sets of mesh systems were built, with the numbers of cells being 1,259,490, 1,695,378 and 2,147,981 respectively. The grid-independence test showed that the difference between the two mesh systems with 1,695,378 and 2,147,981 cells was negligible. Therefore, considering the calculation accuracy and the calculation cost, the mesh system with 1,695,378 cells was selected in this study. Figure 2 shows the mesh of the whole furnace and the mesh of the cross-section near the burner area.

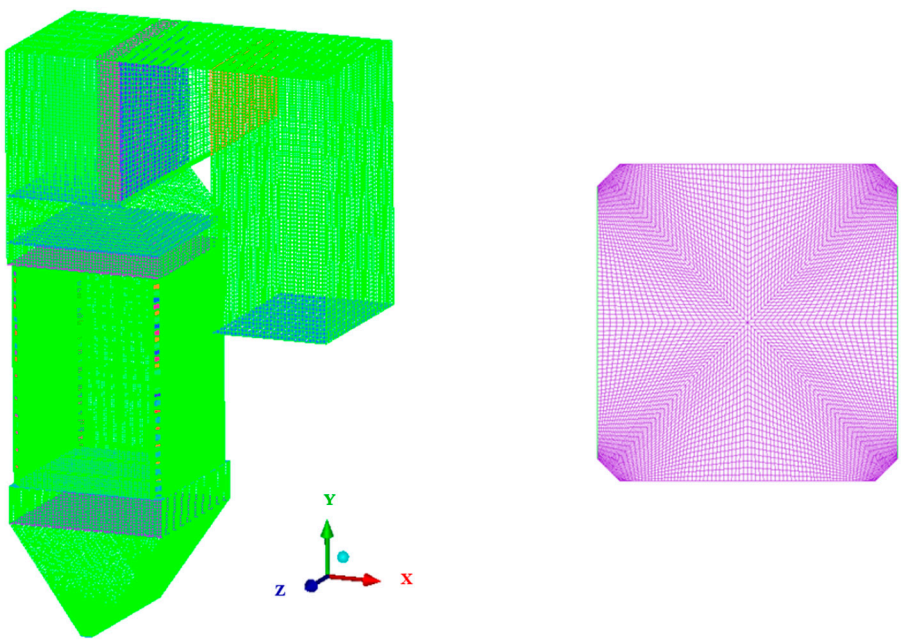

Figure 2. Mesh system of the boiler.

2.2. Coal Parameters and Boundary Conditions

The coal used in this boiler was bituminous coal with a relatively high volatile content. The coal properties coal ash analysis can be found in Tables S1 and S2, respectively, in the Supporting Information. The size of coal particles followed the Rosin–Rammler distribution [24]. The minimum size, the maximum size and the average size of the coal particles were 1 μm, 200 μm and 61 μm, respectively.

This study can be divided into two parts. The first part focuses on the influence of the overall Cl concentration in the furnace; that is, the level of Cl in the coal. The second part focuses on the impacts of introducing a small amount of Cl-containing compounds from SOFA nozzles on mercury species distributions. For all cases studied in this paper, the total excess air ratio and the excess air ratio in the primary zone were set as 1.2 and 0.8, respectively. The coal feeding rate of the boiler was 60.08 $kg \cdot s^{-1}$, and the total air flow rate was 550.85 $kg \cdot s^{-1}$. The temperatures of primary air and secondary air (SA) were kept at 353 K and 612 K, respectively. A mass flow inlet boundary was adopted for air nozzles during the calculation. More details about the operating conditions and the nozzle sizes are listed in Table 1.

Table 1. Operating parameters and boundary conditions.

Parameters	Unit	Value
coal feeding rate	$kg \cdot s^{-1}$	60.0833
theoretical air requirement	$kg \cdot kg^{-1}$	7.6401
total excess air ratio	-	1.2
excess air ratio in the primary zone	-	0.8
total air flow rate	$kg \cdot s^{-1}$	550.8512
PA rate	-	0.29
SA rate	-	0.51
SOFA rate	-	0.40
PA temperature	K	353
SA temperature	K	612
PA density	$kg \cdot m^{-3}$	1.0000
SA density	$kg \cdot m^{-3}$	0.5768
Length of PA nozzles	mm	516
Height of UFA nozzles	mm	218
Height of CCOFA nozzles	mm	254
Height of SOFA nozzles	mm	490

3. Computational Modeling

3.1. Coal Combustion and NO_x Formation

The combustion of coal is a complicated process, including preheating, drying, volatile release, ignition, combustion of volatiles, combustion of char and burnout, along with other physical and chemical processes, such as multiphase flow, heat radiation and heat convection. In this paper, FLUENT was used to simulate the flow, heat transfer and combustion processes in the furnace. The fluid flow was described using the standard k-ε model, which has been widely used in the calculation of flow fields in boiler furnaces [25]. The two-competing-rate model was adopted to calculate the release of volatiles while the kinetic–diffusion-limited rate model was selected to calculate the char combustion process [26]. Additionally, the turbulent dispersion of coal particles was predicted using a stochastic tracking approach. The radiative transfer equation inside the furnace was solved using the discrete ordinate (DO) radiation model. The non-premixed combustion process was simplified and solved by applying the assumed-shape probability density function (PDF) approach [27]. As for the pressure–velocity coupling, the phase-coupled SIMPLE (PC-SIMPLE) algorithm was used to solve the equations [28]. After obtaining the velocity field, temperature field and concentration field of flue gas components in the furnace, the distributions of nitrogen oxides species were then calculated. The main species of nitrogen

oxides generated during coal combustion are NO and NO_2, among which NO accounts for more than 90%. In addition, a small amount of N_2O is formed. According to the formation path, NO_x can be divided into thermal NO_x, fuel NO_x and prompt NO_x. In terms of coal-fired boilers, thermal NO_x and fuel NO_x are dominant while prompt NO_x is negligible [29]. In this study, the formation of thermal NO_x was described using the Zeldovich mechanism. The fuel NO_x was generated from volatile nitrogen and char nitrogen, with HCN and NH_3 as the important intermediate products during the reaction.

3.2. Homogeneous Oxidation of Hg^0

Based on the simulation results of coal combustion and NO_x formation, the homogeneous oxidation process of Hg^0 was calculated using the eddy dissipation concept (EDC) model. The EDC model takes into account the specific chemical reaction mechanism in turbulence, which assumes that all chemical reactions take place in a very small turbulent structure [30,31]. It should be mentioned that tabulated chemistry modeling has been used by several researchers as an alternative method to EDC in some cases for better combination with the detailed mechanisms [32–34]. However, the accuracy of these gaseous flamelet-based tabulated chemistry models would be reduced for coal combustion cases because the large coal particles may pass through the flame surface during the combustion process. Additionally, in order to consider the slow chemical processes, such as the generation of pollutants (Hg, NO_x, SO_x, etc.), the tabulated chemistry models need to be further extended to the unsteady form. Hence, we use the EDC model to carry out the numerical study for Hg reactions within the coal-fired utility boiler.

The homogeneous oxidation of Hg^0 in coal-fired boilers is very complicated and affected by many factors, such as the temperature distribution and concentration of flue gas components. Moreover, as there is no sub-model for Hg reaction in FLUENT, a new Hg model must be built and imported for calculation. Some scholars believe that the reactions between mercury and chlorine are the most important for the homogeneous reaction of mercury. Based on this, a set of kinetic model containing 8 reversible elementary reactions was proposed [35]. Sliger et al. proposed that the most important factors affecting the homogeneous reaction of Hg were the HCl concentration, flue gas cooling rate and background gas composition, and found that the reaction between Hg and Cl was the main pathway for the oxidation of Hg^0 [15]. The findings of Xu et al. showed that oxygen also plays a key role in the homogeneous reaction of mercury in addition to chlorine. Therefore, a kinetic model for homogeneous reactions of Hg was proposed, including HgO-related elemental reactions [36]. According to the results of the sensitivity analysis, the reaction of Hg + ClO = HgO + Cl is as important as the widely used reactions of Hg + Cl_2 = HgCl + Cl and Hg + HCl = HgCl + H.

Based on these previous studies, a novel Hg sub-model was proposed to achieve the coupling of thermodynamics, reaction kinetics and fluid dynamics for the homogeneous reactions of Hg in a full-scale boiler. Here, 32 elementary reactions were selected to describe the homogeneous oxidation process of Hg^0 in a coal-fired utility boiler. The kinetic parameters of the reactions were obtained from the literature and have been verified in experimental studies [15]. The thermodynamic data for Hg and HgCl were obtained from the NIST database and imported into CHEMKIN together with elemental reactions. Then, the che file (shown in Table S2 in the Supporting Information), which can be used as the source file for the Hg sub-model in FLUENT, was generated by FitDat.

4. Results and Discussion

4.1. Model Validation

In order to validate the model used in this study, the simulation results were compared with the practical measured data from the coal-fired power plant. As shown in Figure 3, the flue gas temperature and the O_2 concentration at the furnace outlet, the wall heat flux, the carbon content in fly ash and the NO_x emission were selected for comparison and validation. The largest error occurred in the carbon content in fly ash, with a relative error

of 7.56%. The relative errors of the temperature of the furnace outlet, O_2 concentration at the furnace outlet, the wall heat flux and the NO_x emission were 2.70%, 3.62%, 3.35% and 1.41%, respectively, which are acceptable results for the practical application of coal-fired utility boilers [37]. Hence, the model adopted in this study can simulate the flow, combustion and heat transfer processes well. In terms of the Hg distribution, the model was validated by comparing the simulation results with the findings from the literature, which can be found in Section 4.3, together with the discussion on the homogeneous reactions of Hg.

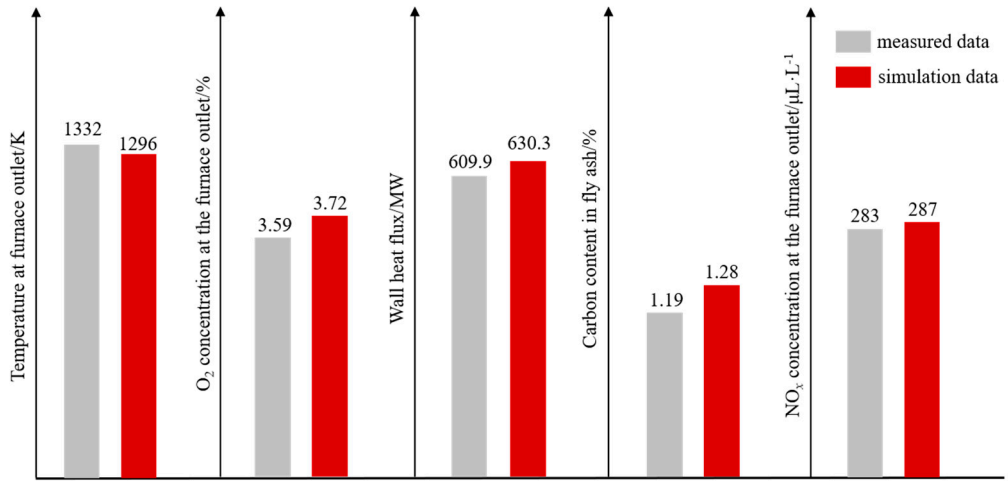

Figure 3. Model validation.

4.2. Simulation Results before Considering Hg Reactions

Before importing the mercury sub-model, the combustion process in the boiler was calculated using the non-premixed combustion model. After the temperature distribution, velocity distribution and flue gas components distribution were obtained, the NO_x model was activated. An imaginary coordinate was established within the boiler, which started from the bottom of the hopper and ended at the outlet of the calculation zone. A cross-section perpendicular to the coordinate was built every 1 m along the axis. The average flue gas temperature on each cross-section was calculated, with the results shown in Figure 4. It can be seen that the coordinate axis passed through the hopper area, the primary zone, the burnout area, the horizontal flue pass and the vertical flue pass. The fuel was injected into the furnace at the primary zone and mixed with the PA and SA, resulting in the intense combustion reaction and the rapid rise in flue gas temperature. Figure 5 shows the temperature contour of the cross-section at 25 m, from which it can be seen that the ideal tangential combustion was formed in the primary zone. In the burnout zone, the introducing of SOFA caused further combustion of the unburned carbon, so the temperature of the flue gas increased again. Then, the temperature of the flue gas dropped gradually because of the heat transfer between the flue gas and the water wall or other heat exchangers.

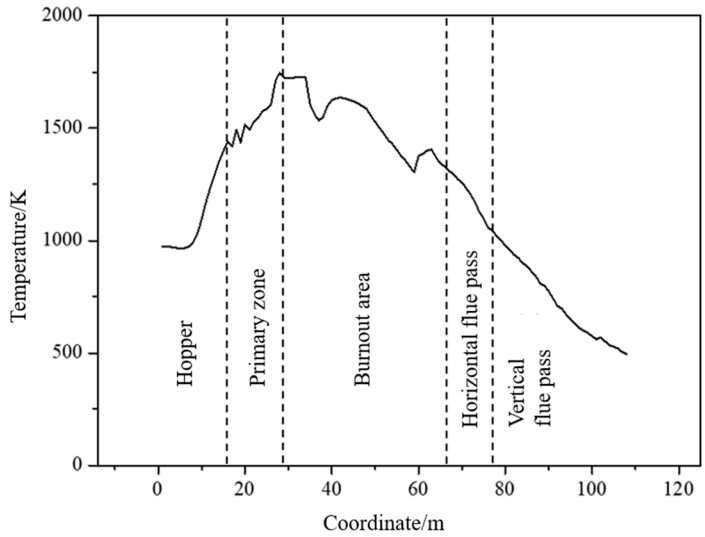

Figure 4. Flue gas temperature along the coordinates.

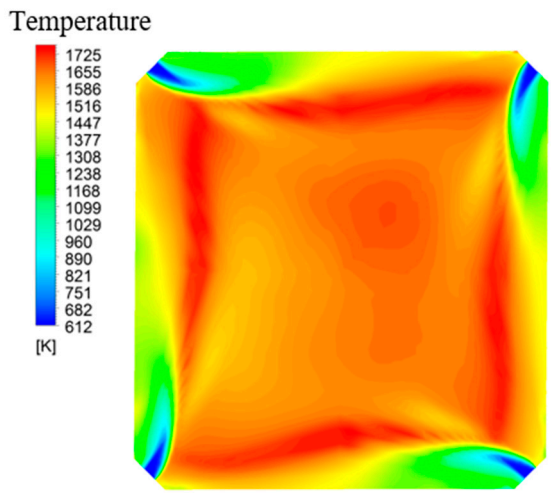

Figure 5. Temperature contour of the cross-section in the primary zone.

Figure 6 shows the velocity contour and distributions of the main flue gas components (including O_2, CO_2, H_2O and NO) within the boiler. As can be seen from Figure 6a, the flow field in the furnace showed good symmetry. The maximum velocity appeared in the vicinity of the nozzles, especially near the SOFA nozzles, while the flue gas velocity in the furnace center was relatively lower. The O_2 carried by PA and SA was mainly consumed in the primary zone, leading to the lower O_2 mole concentration in the center of the furnace, as shown in Figure 6b. Part of the O_2 was added through the SOFA nozzles for the oxidation of unburned carbon and CO, after which the O_2 concentration decreased gradually. Figure 6c presents the distribution of CO_2. As the main product of coal combustion, the distribution of CO_2 was almost opposite to that of O_2. The H_2O distribution is shown in Figure 6d. The release of the moisture in coal and the reaction of the H element during the combustion process were the main sources of H_2O within the boiler. The H_2O concentration was higher near the nozzles and in the primary zone, while lower in the central area of the burnout zone. H_2O can react with chlorine to form OH through the equation of Cl + H_2O = OH + HCl, which would participate in the Hg-related reactions. Therefore, it is necessary to consider the distribution of H_2O in the furnace before the calculation of the Hg model. Similarly, nitrogen oxides could also be involved in the homogeneous reactions of mercury. The distribution of NO is shown in Figure 6e. The highest concentration of NO can be observed in the vicinity of the nozzles in the primary zone.

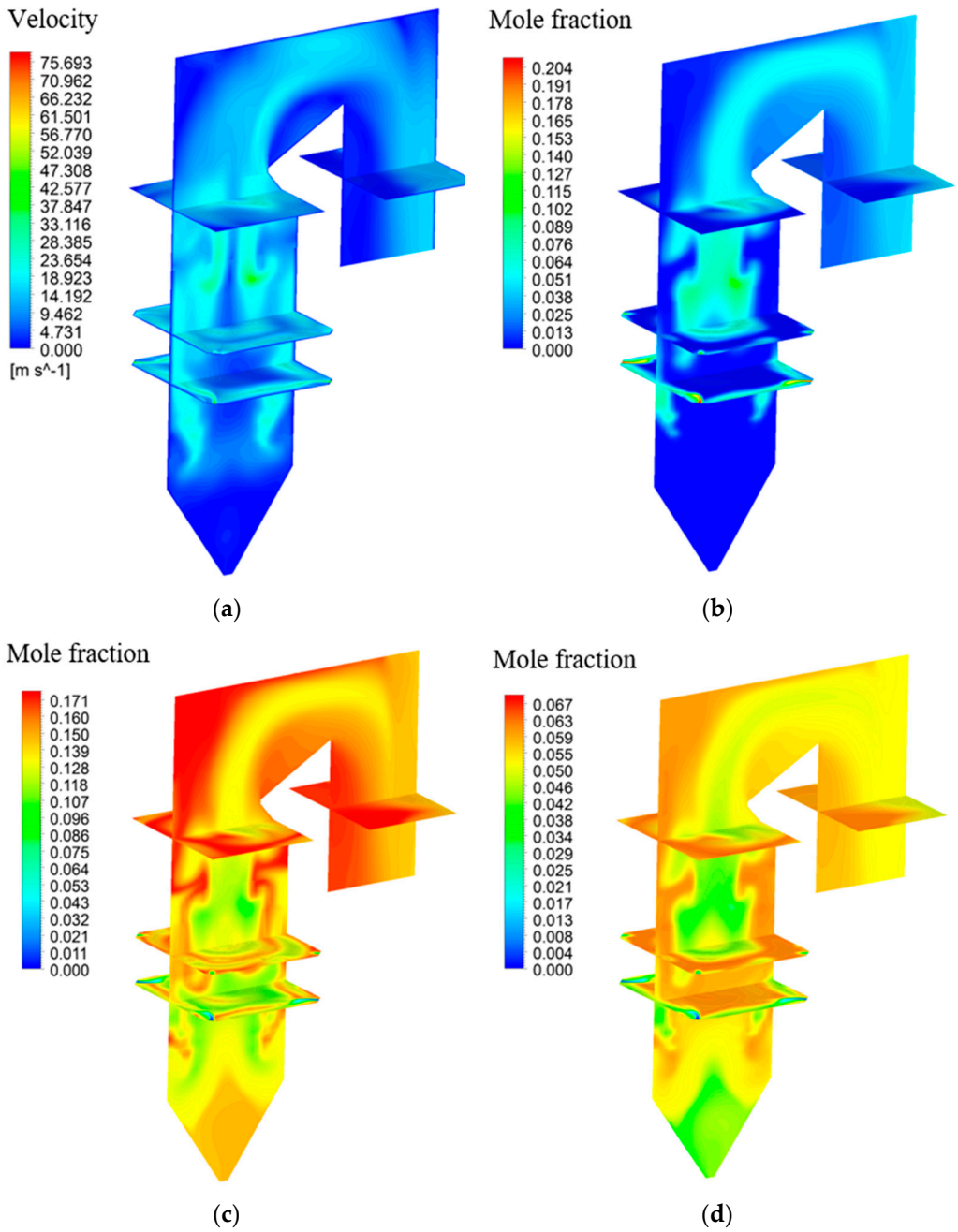

Figure 6. *Cont.*

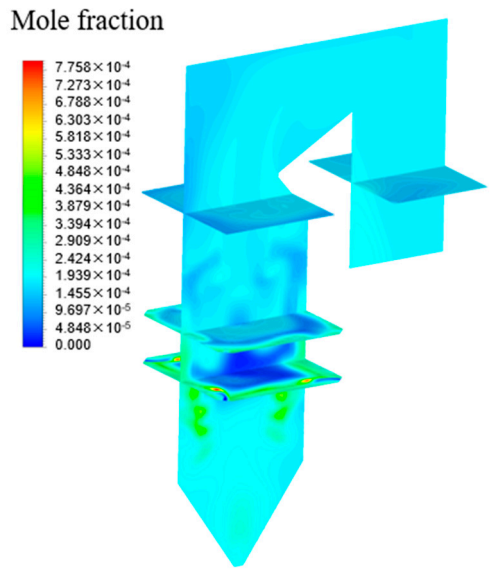

(e)

Figure 6. Velocity contour and distributions of the main flue gas components: (**a**) velocity contour; (**b**) O_2 mole fraction; (**c**) CO_2 mole fraction; (**d**) H_2O mole fraction; (**e**) NO mole fraction.

4.3. Effects of Chlorine Content in Coal on Homogeneous Reactions of Hg

Based on the results in Section 4.2, the homogeneous reactions of mercury species in coal-fired boilers were studied by utilizing the mercury sub-model. The reason why the Hg-related homogeneous reactions can be calculated using the post-treatment approach is that the contents of mercury species are very low. The mole concentrations of mercury species are orders of magnitude lower than those of other main flue gas components, such as O_2, CO_2, H_2O and NO, which means the influences of mercury-related reactions on the distributions of other flue gas components are negligible. In other word, the obtained simulation results in Section 4.2 are still applicable after considering the mercury sub-model.

Since the reactions between Hg and Cl are vital in the homogeneous oxidation of Hg^0, it is of great significance to study the effects of chlorine content in coal on the distributions of mercury species in coal-fired boilers [38]. Previous studies have shown that the Cl element in coal would be released in the form of HCl after entering the furnace [39]. Additionally, Hg^0 is the dominant mercury species under the high-temperature conditions of the primary zone. Therefore, HCl and Hg^0 were introduced from the PA nozzles when setting boundary conditions. Two cases (case A and case B) were set up with various chlorine contents in coal. Specifically, low-chlorine coal was used in case A, while high-chlorine coal was used in case B. The concentration of HCl in PA was set as 100 $\mu L \cdot L^{-1}$ in case A, which meant the Cl content in the coal in case A was 270 $mg \cdot kg^{-1}$. The average concentration of HCl in the boiler can be calculated using Equations (1)–(7):

$$C_A(\mathrm{HCl}) = C_{A1}(\mathrm{HCl}) \times (V_1/V) \times (V/V_y) \tag{1}$$

$$V = \alpha \times V_0 \tag{2}$$

$$V_y = V_{\mathrm{RO_2}} + V_{\mathrm{H_2O}} + V_{\mathrm{N_2}} + V_{\mathrm{O_2}} \tag{3}$$

$$V_{\mathrm{RO_2}} = 0.01866 \times (\mathrm{C_{ar}} + 0.375\mathrm{S_{ar}}) \tag{4}$$

$$V_{\mathrm{H_2O}} = 0.111\mathrm{H_{ar}} + 0.0124\mathrm{M_{ar}} + 0.0161V_0 \tag{5}$$

$$V_{\mathrm{N_2}} = 0.79\alpha V_0 + 0.008\mathrm{N_{ar}} \tag{6}$$

$$V_{\mathrm{O_2}} = 0.21 \times (\alpha - 1)V_0 \tag{7}$$

where C_A(HCl) represents the average concentration of HCl in the boiler for case A, C_{A1}(HCl) represents the concentration of HCl in PA for case A, V_1 represents the flow rate of PA, V represents the total air flow rate, V_0 represents the theoretical air flow rate and V_y represents the flow rate of flue gas. Combined with the parameters in Table S1 and Table 1, it can be calculated that C_A(HCl) was about 23.5 μL·L^{-1}. In case B, the concentration of HCl in PA was set as 400 μL·L^{-1}, which meant the Cl content in the high-Cl coal was 1080 mg·kg^{-1}. By replacing Equation (1) with the following equation, the average concentration of HCl in the boiler for case B can be obtained:

$$C_B(\mathrm{HCl}) = C_{B1}(\mathrm{HCl}) \times \frac{V_1}{V} \times \frac{V}{V_y} \tag{8}$$

where C_B(HCl) represents the average concentration of HCl in the boiler for case B and C_{B1}(HCl) represents the concentration of HCl in PA for case B. The value of C_B(HCl) was about 94.0 μL·L^{-1}. In addition, the total mercury concentration in the boiler was set at 60 μg·m^{-3} in both case A and case B. The Hg content in the coal can be calculated as 0.567 mg·kg^{-1} in this study.

Figures 7–9 show the distributions of chlorine species in the boiler under various cases. It should be mentioned here based on case A that case C was set up with 200 μL·L^{-1} of HCl fed into the SOFA nozzles on the third layer (five layers of SOFA nozzles in total). The detailed results of case C will be discussed later on (Section 4.4). In this section, we only focus on the simulation results of case A and case B. Besides HCl, the concentrations of Cl and Cl_2 in case B were also obviously higher than those in case A. Comparing the concentrations of these species, HCl is the dominant form of chlorine species in the whole furnace. The distributions of mercury species in the furnace are presented in Figures 10–13. The contours show that the homogeneous oxidation of Hg^0 in the coal-fired boiler mainly occurred in the vertical flue pass, where the temperature was relatively lower. Because of the high temperature in the furnace zone, the concentrations of oxidized mercury species were at least two orders of magnitude lower than that of Hg^0. At the exit of the boiler, Hg^0 was still the dominant Hg-containing species, while $HgCl_2$ had the highest concentration among the oxidized mercury species. These results are in good agreement with the experimental data from the literature, indicating that the Hg sub-model used in this paper can simulate the homogeneous reactions of mercury in the furnace accurately [15,39].

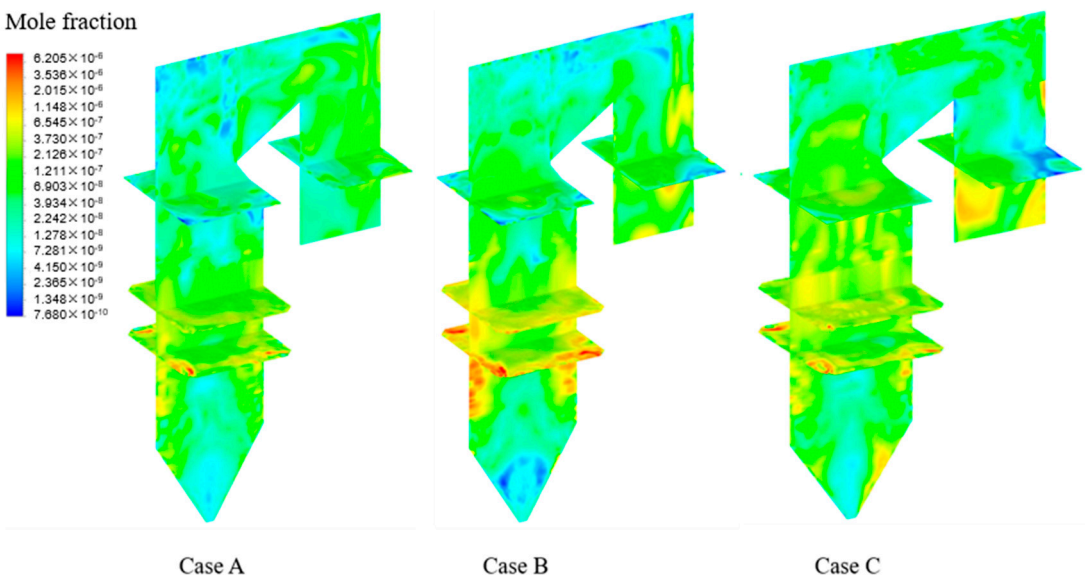

Figure 7. Distribution of Cl in various cases.

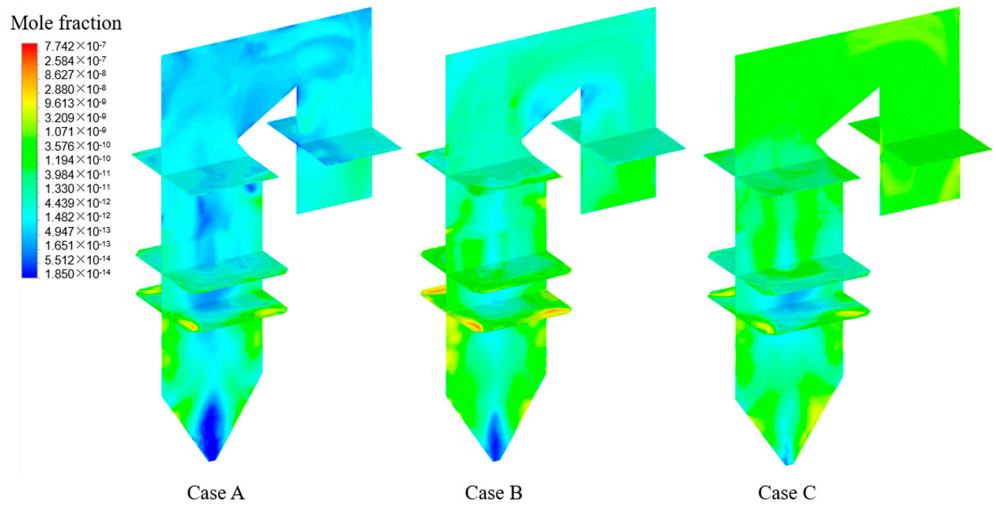

Figure 8. Distribution of Cl_2 in various cases.

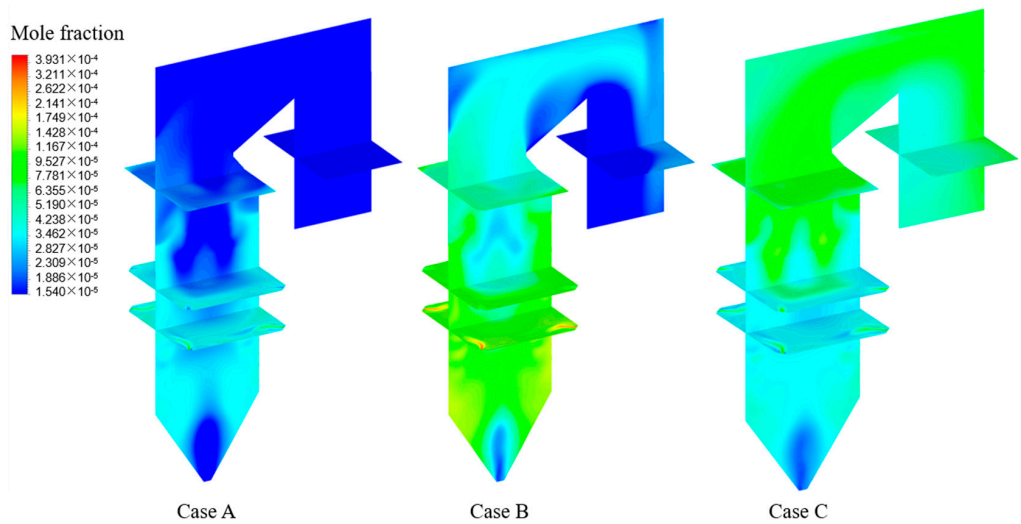

Figure 9. Distribution of HCl in various cases.

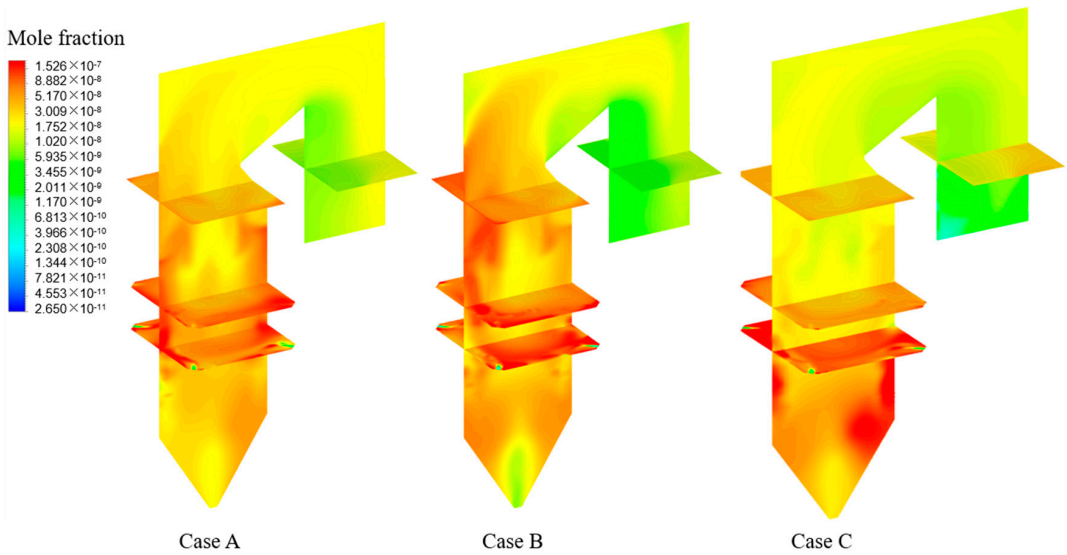

Figure 10. Distribution of Hg^0 in various cases.

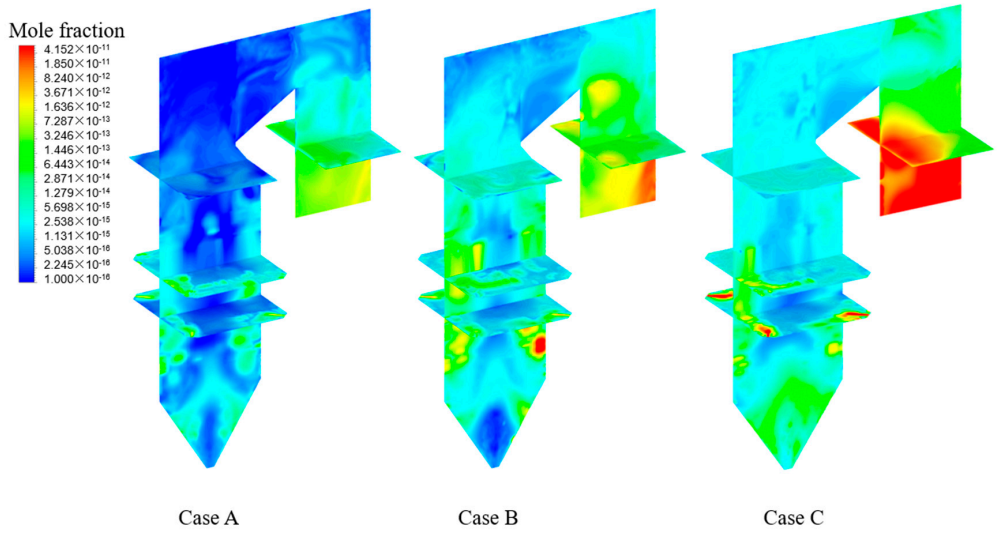

Figure 11. Distribution of HgCl in various cases.

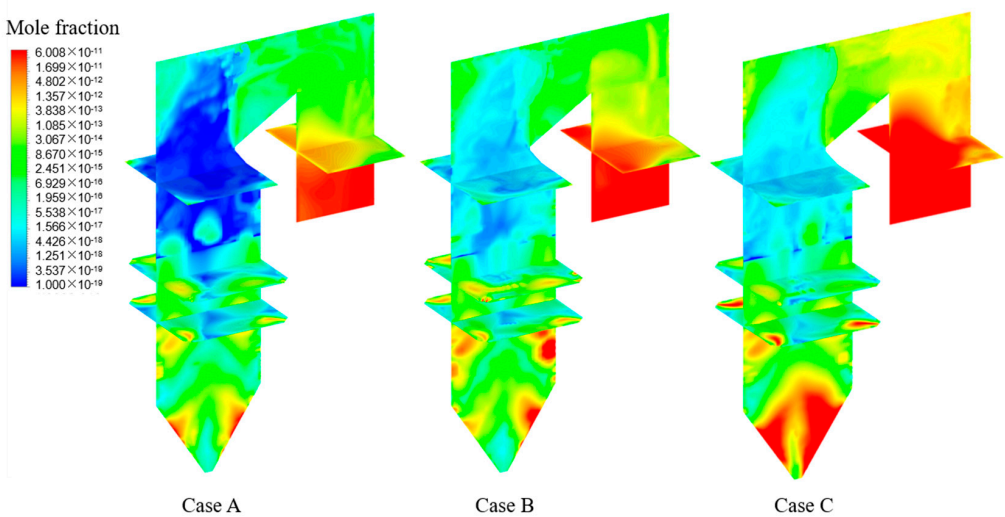

Figure 12. Distribution of $HgCl_2$ in various cases.

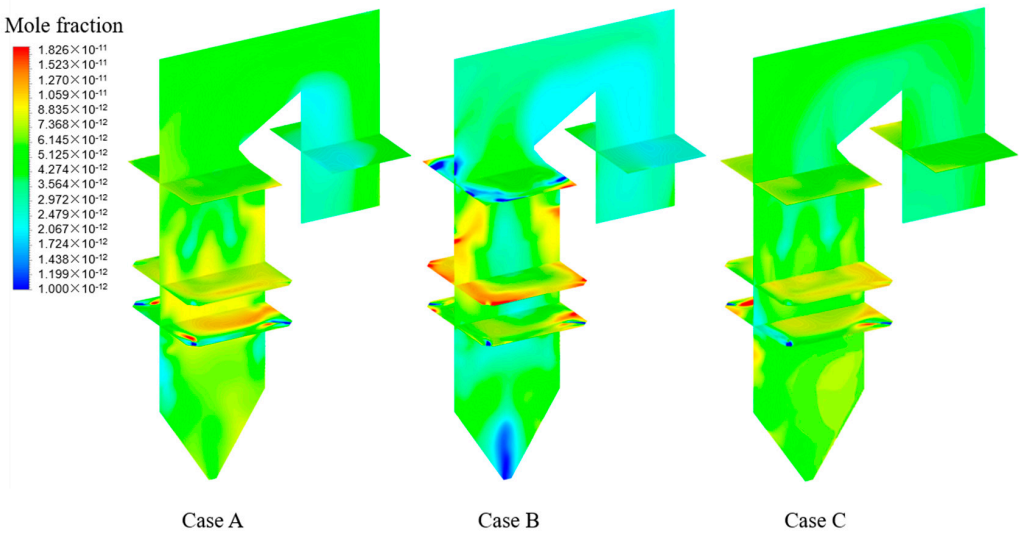

Figure 13. Distribution of HgO in various cases.

The concentration of Hg^0 was higher in the lower part of the furnace, which is consistent with the findings of Zhang et al. [39]. This can be attributed to the large relative atomic mass of Hg. As the flue gas flowed to the upper part of the furnace, the horizontal flue pass and the vertical flue pass, the temperature of the flue gas also gradually decreased. The homogeneous oxidation of Hg^0 then occurred, especially in the vertical flue pass.

In order to analyze the influence of chlorine content in coal on homogeneous reactions of Hg quantitatively, the ratios of Hg and its compounds at the boiler outlet were calculated, as listed in Table 2. In spite of the intense oxidation reactions of Hg^0, the concentration of Hg^0 remained above 90% in the vertical flue pass. Comparatively, the ratios of Hg^0 in case A and case B were 99.039% and 95.196%, respectively, which meant more Hg^0 underwent homogeneous oxidation in the case with higher Cl content in coal.

Table 2. Ratios of Hg species at the boiler outlet in various cases.

Case	Hg^0	HgCl	$HgCl_2$	HgO
A	99.039	0.008	0.922	0.031
B	95.196	0.041	4.746	0.017
C	84.145	0.596	15.239	0.020

The proportion of $HgCl_2$ in oxidized mercury is shown in Figure 14 to better analyze the composition of the oxidized mercury. It can be seen that $HgCl_2$ was the main component among the oxidized mercury species, which is consistent with the findings in the contours. The proportions of $HgCl_2$ were higher than 95.9% in both cases. The results confirm that chlorine plays an important role in homogeneous oxidation of Hg^0 in coal-fired boiler [40].

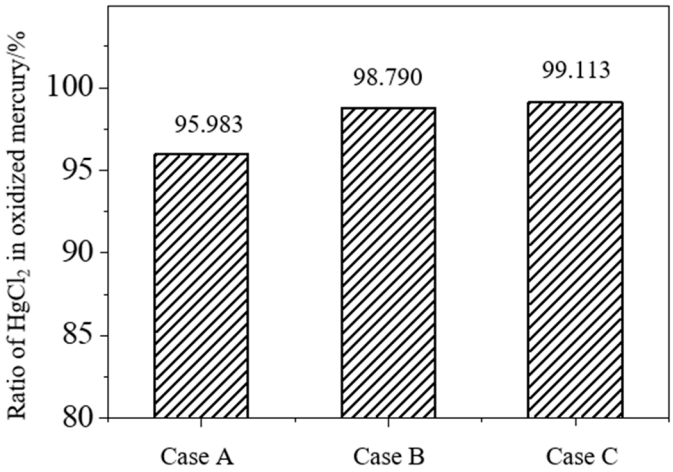

Figure 14. The proportion of $HgCl_2$ in oxidized mercury species in various cases.

4.4. Effects of Adding HCl on Homogeneous Reactions of Hg

Considering the important role of Cl-containing compounds in homogeneous reactions of Hg, a small amount of HCl can be added into boilers to promote the oxidation of Hg^0. Nevertheless, the quantitative influence of HCl addition on the homogeneous reactions of Hg in full-scale utility boilers remains unclear. In this section, the distributions of chlorine-containing and mercury-containing species in the boiler before and after adding HCl are studied. According to the above analyses, the homogeneous reactions of Hg hardly occurred in the primary zone. Hence, supplementary HCl was added through the SOFA nozzles in the burnout area (case C). Combining Equations (2)–(7) and Equation (9), it can be calculated that the average concentration of HCl in the boiler in case C was about

39.7 μL·L^{-1}, which was about 69% higher than that in case A, but still lower than in case B. The concentration of Hg was kept at 60 μg·m^{-3} in case C.

$$C_C(\mathrm{HCl}) = C_A(\mathrm{HCl}) + C_{\mathrm{SOFA-3}}(\mathrm{HCl}) \times \frac{V_{\mathrm{SOFA-3}}}{V} \times \frac{V}{V_y} \tag{9}$$

where C_C(HCl) represents the average concentration of HCl in the boiler for case C, $C_{\mathrm{SOFA-3}}$(HCl) represents the concentration of HCl in the third layer of SOFA nozzles and $V_{\mathrm{SOFA-3}}$ represents the air flow rate from the third layer of SOFA nozzles.

As shown in Figures 7–9, the concentrations of Cl-containing species in case C were significantly higher than those in case A, especially in the burnout area. HCl was still the dominant component, while the concentration of Cl_2 was the lowest. Figures 10–13 depict the contours of the Hg-containing species. The concentration of Hg^0 in the burnout area was reduced significantly after the addition of HCl. In the whole boiler, especially in the vertical flue pass, the concentrations of $HgCl_2$ and HgCl increased remarkably in case C, while the impact of HCl addition on HgO was relatively slight. As the removal of elemental mercury is much more difficult than that of oxidized mercury, HCl addition is beneficial for Hg pollution control from coal-fired power plants burning low-Cl coal [41].

According to Table 2, after the addition of HCl, the ratio of Hg^0 decreased from 99% to about 84%, while the ratio of $HgCl_2$ increased by over 16 times and the content of HgCl also increased significantly. It is worth noting that the ratio of Hg^0 in case C is even lower than that in case B, which indicates that the homogeneous oxidation of Hg^0 in case C was more intense than that in case B, although the average Cl concentration in the boiler was lower. Therefore, it can be concluded that the addition of a small amount of HCl from the burnout area had an obvious promotion effect on the homogeneous oxidation of Hg^0.

Zhuang et al. have experimentally studied the influence of adding $CaCl_2$ on the oxidation of Hg^0 in boilers [41]. They found that adding 600~1000 μL·L^{-1} $CaCl_2$ would increase the concentration of chlorine in flue gas by 88.0~146.7 μL·L^{-1}. They reported that this level of chlorine concentration was common for boilers using high-Cl bituminous coal and would not cause serious corrosion problems. In this study, the average chlorine concentrations of flue gas in the three cases were 23.5 μL·L^{-1}, 94.0 μL·L^{-1} and 39.7 μL·L^{-1}, respectively. Compared with the results from Zhuang et al. [41], the Cl concentration in this paper was acceptable for practical engineering applications. Therefore, adding HCl into boilers fired with low-Cl coal can promote the homogeneous oxidation of Hg^0 significantly without causing serious corrosion problems.

5. Conclusions

A numerical study was conducted on the homogeneous reactions of mercury in a coal-fired utility boiler. For the first time, a novel mercury sub-model was built in a full-scale tangentially coal-fired boiler to achieve the coupling of thermodynamics, reaction kinetics and fluid dynamics. Since Cl is the most important element in the homogeneous oxidation of Hg^0, the influence of the Cl content in coal on the homogeneous reaction of Hg in a boiler was studied. In addition, the quantitative effect of adding HCl on the homogeneous reactions of Hg within a full-scale boiler fired with low-Cl coal was investigated, which has not been reported before. The following conclusions can be drawn:

1. Ideal tangential combustion was achieved in the primary zone, causing the flue gas temperature to rise rapidly to 1748 K. The velocity field showed good symmetry in the furnace. The concentrations of H_2O (~0.06 in mole fraction) and NO (~7×10^{-4} in mole fractions) were higher in the vicinity of the primary air nozzles;

2. More elemental mercury (~4.8%) was converted to oxidized mercury through homogeneous reactions when high-Cl coal was burned, which is conducive to mercury pollution control. HCl was the main component of chlorine species in the boiler, while the concentrations of Cl and Cl_2 were low. The homogeneous reactions of Hg mainly occurred in the vertical flue pass with lower temperature. At the boiler exit, Hg^0 remained

the dominant (>95.2%) Hg-containing species, while $HgCl_2$ accounted for the largest proportion (>95.9%) of the oxidized mercury;

3. Adding HCl from the separated overfire air nozzles can promote the homogeneous oxidation of Hg^0 remarkably. The ratio of $HgCl_2$ increased by over 16 times. It is worth noting that even after introducing HCl into the boilers using low-Cl coal, the average concentration of HCl (39.7 $\mu L \cdot L^{-1}$) was still lower than the common cases when high-Cl coal was fired. Hence, adding HCl is a safe and effective method of Hg pollution control from the perspectives of chlorine corrosion and Hg^0 oxidation.

In general, the results of this study are of significance in understanding the homogeneous reactions between Hg and Cl within a full-scale utility boiler. The methodology used in this numerical work paves the way for the further development of advanced Hg models. The combination of detailed tabulated chemistry modeling and coal combustion deserves more attention in the future.

Supplementary Materials: The following are available online at https://www.mdpi.com/article/10.3390/en15020446/s1: Table S1: Coal properties. Table S2: Coal ash composition analysis. Table S3. Source file of Hg sub-model.

Author Contributions: Conceptualization, Q.L.; methodology, Q.L.; software, Q.L. and X.L.; validation, X.L.; investigation, Q.L.; resources, C.W.; data curation, Q.L.; writing—original draft preparation, Q.L.; writing—review and editing, C.W.; supervision, C.W.; project administration, D.C.; funding acquisition, Q.L. All authors have read and agreed to the published version of the manuscript.

Funding: This work was supported by the Science and Technology Project of Beilin District, Xi'an (No. GX2120).

Conflicts of Interest: The authors declare no conflict of interest.

References

1. Fernández-Miranda, N.; Rodríguez, E.; Lopez-Anton, M.A.; García, R.; Martínez-Tarazona, M.R. A new approach for retaining mercury in energy generation processes: Regenerable carbonaceous sorbents. *Energies* **2017**, *10*, 1311. [CrossRef]
2. Lv, Q.; Cai, M.; Wang, C.A.; He, Y.; Che, D.F. Investigation on elemental mercury removal by cerium modified semi-coke. *J. Energy Inst.* **2020**, *93*, 666–678. [CrossRef]
3. Li, X.; Teng, Y.; Zhang, K.; Peng, H.; Cheng, F.; Yoshikawa, K. Mercury migration behavior from flue gas to fly ashes in a commercial coal-fired CFB power plant. *Energies* **2020**, *13*, 1040. [CrossRef]
4. Yang, Y.; Liu, J.; Wang, Z. Reaction mechanisms and chemical kinetics of mercury transformation during coal combustion. *Prog. Energ. Combust.* **2020**, *79*, 100844. [CrossRef]
5. Contreras, M.L.; Ganesh, N.; Rodilla, I.; Bahillo, A. Assess of biomass co-firing under oxy-fuel conditions on Hg speciation and ash deposit formation. *Fuel* **2018**, *215*, 395–405. [CrossRef]
6. Galbreath, K.C.; Zygarlicke, C.J. Mercury transformations in coal combustion flue gas. *Fuel Process. Technol.* **2000**, *65*, 289–310. [CrossRef]
7. Senior, C.L.; Sarofim, A.F.; Zeng, T.F.; Helble, J.J.; Mamani-Paco, R. Gas-phase transformations of mercury in coal-fired power plants. *Fuel Process. Technol.* **2000**, *63*, 197–213. [CrossRef]
8. Frandsen, F.; Dam-Johansen, K.; Rasmussen, P. Trace elements from combustion and gasification of coal—An equilibrium approach. *Prog. Energ. Combust.* **1994**, *20*, 115–138. [CrossRef]
9. Chen, L.; Duan, Y.; Zhuo, Y.; Yang, L.G.; Zhang, L.; Yang, X.H.; Yao, Q.; Jiang, Y.M.; Xu, X.C. Mercury transformation across particulate control devices in six power plants of China: The co-effect of chlorine and ash composition. *Fuel* **2007**, *86*, 603–610.
10. Ito, S.; Yokoyama, T.; Asakura, K. Emissions of mercury and other trace elements from coal-fired power plants in Japan. *Sci. Total Environ.* **2006**, *368*, 397–402. [CrossRef] [PubMed]
11. Pavlish, J.H.; Holmes, M.J.; Benson, S.A.; Crocker, C.R.; Galbreath, K.C. Application of sorbents for mercury control for utilities burning lignite coal. *Fuel Process. Technol.* **2004**, *85*, 563–576. [CrossRef]
12. Laudal, D.L.; Brown, T.D.; Nott, B.R. Effects of flue gas constituents on mercury speciation. *Fuel Process. Technol.* **2000**, *65*, 157–165. [CrossRef]
13. Wang, J.S.; Clements, B.; Zanganeh, K. An interpretation of flue-gas mercury speciation data from a kinetic point of view. *Fuel* **2003**, *82*, 1009–1011. [CrossRef]
14. Jiao, Y.; Dibble, T.S. First kinetic study of the atmospherically important reactions BrHg+NO_2 and BrHg+HOO. *Phys. Chem. Chem. Phys.* **2017**, *19*, 1826–1838. [CrossRef]
15. Sliger, R.N.; Kramlich, J.C.; Marinov, N.M. Towards the development of a chemical kinetic model for the homogeneous oxidation of mercury by chlorine species. *Fuel Process. Technol.* **2000**, *65*, 423–438. [CrossRef]

16. Galbreath, K.C.; Zygarlicke, C.J.; Tibbetts, J.E.; Schulz, R.L.; Dunham, G.E. Effects of NO_x, α-Fe_2O_3, γ-Fe_2O_3, and HCl on mercury transformations in a 7-kW coal combustion system. *Fuel Process. Technol.* **2004**, *86*, 429–448. [CrossRef]
17. Wang, F.; Li, G.; Wang, S.; Wu, Q.; Zhang, L. Modeling the heterogeneous oxidation of elemental mercury by chlorine in flue gas. *Fuel* **2020**, *262*, 116506. [CrossRef]
18. Lv, Q.; Wang, C.A.; He, Y.; Cai, M.; Che, D.F. Elemental mercury removal over CeO_2/TiO_2 catalyst prepared by sol–gel method. *Appl. Sci.* **2020**, *10*, 2706. [CrossRef]
19. Zhao, L.; Wu, Y.W.; Han, J.; Wang, H.X.; Liu, D.J.; Lu, Q.; Yang, Y.P. Density functional theory study on mechanism of mercury removal by CeO_2 modified activated carbon. *Energies* **2018**, *11*, 2872. [CrossRef]
20. Ma, L.; Chen, X.; Liu, J.; Fang, Q.; Zhang, C.; Li, Y.; Mao, R.; Ren, L.; Zhang, P.; Chen, G. Insights into the causes and controlling strategies of gas temperature deviation in a 660 MW tangentially fired tower-type boiler. *Appl. Therm. Eng.* **2021**, *196*, 117297. [CrossRef]
21. Liu, X.; Zhang, J.; Tan, H.; Mo, Q.; Wang, X.; Wang, Y. Numerical and experimental study on co-firing of low volatile coal in a 330 MW tangentially fired boiler. *J. Energy Inst.* **2021**, *96*, 242–250. [CrossRef]
22. Sankar, G.; Chandra, S.D.; Santhosh, K.D.; Balasubramanian, K.R. Numerical simulation of the heat transfer and NO_x emissions in a 660 MW tangentially fired pulverised-coal supercritical boiler. *Heat Mass Transfer* **2020**, *56*, 2693–2709.
23. Jiang, Y.; Lee, B.-H.; Oh, D.-H.; Jeon, C.-H. Optimization of operating conditions to achieve combustion stability and reduce NO_x emission at half-load for a 550-MW tangentially fired pulverized coal boiler. *Fuel* **2021**, *306*, 121727. [CrossRef]
24. Che, D. *Boilers-Theory, Design and Operation*, 1st ed.; Xi'an Jiaotong University Press: Xi'an, China, 2008; p. 245.
25. Vuthaluru, R.; Vuthaluru, H.B. Modelling of a wall fired furnace for different operating conditions using FLUENT. *Fuel Process. Technol.* **2006**, *87*, 633–639. [CrossRef]
26. Hurt, R.; Sun, J.K.; Lunden, M. A kinetic model of carbon burnout in pulverized coal combustion. *Combust. Flame* **1998**, *113*, 181–197. [CrossRef]
27. Haas, J.; Tamura, M.; Weber, R. Characterization of coal blends for pulverized fuel combustion. *Fuel* **2001**, *80*, 1317–1323. [CrossRef]
28. Vasquez, S.A.; Ivanov, V.A. A Phase Coupled Method for Solving Multiphase Problems on Unstructured Meshes. In Proceedings of the ASME 2000 Fluids Engineering Division Summer Meeting, Boston, MA, USA, 11–15 June 2000.
29. Hill, S.C.; Smoot, L.D. Modeling of nitrogen oxides formation and destruction in combustion systems. *Prog. Energ. Combust.* **2000**, *26*, 417–458. [CrossRef]
30. Magnussen, B.F. On the Structure of Turbulence and a Generalized Eddy Dissipation Concept for Chemical Reaction in Turbulent Flow. In Proceedings of the 19th Aerospace Sciences Meeting, St. Louis, MO, USA, 12–15 January 1981.
31. Gran, I.R.; Magnussen, B.F. A numerical study of a bluff-body stabilized diffusion flame. Part 2. Influence of combustion modeling and finite-rate chemistry. *Combust. Sci. Technol.* **1996**, *119*, 191. [CrossRef]
32. Mayrhofer, M.; Koller, M.; Seemann, P.; Prieler, R.; Hochenauer, C. Evaluation of flamelet-based combustion models for the use in a flameless burner under different operating conditions. *Appl. Therm. Eng.* **2021**, *183*, 116190. [CrossRef]
33. Sorrentino, G.; Ceriello, G.; Cavaliere, A.; de Joannon, M.; Ragucci, R. Thermo-chemical manifold reduction for tabulated chemistry modeling. Temperature and dilution constraints for smooth combustion reactors. *Proc. Combust. Inst.* **2021**, *38*, 5393–5402. [CrossRef]
34. Wen, X.; Luo, Y.; Wang, H.; Luo, K.; Jin, H.; Fan, J. A three mixture fraction flamelet model for multi-stream laminar pulverized coal combustion. *Proc. Combust. Inst.* **2018**, *37*, 2901–2910. [CrossRef]
35. Pan, H.Y.; Minet, R.G.; Benson, S.W.; Tsotsis, T.T. Process for converting hydrogen-chloride to chlorine. *Ind. Eng. Chem. Res.* **1994**, *33*, 2996–3003. [CrossRef]
36. Xu, M.H.; Qiao, Y.; Zheng, C.G.; Li, L.C.; Liu, J. Modeling of homogeneous mercury speciation using detailed chemical kinetics. *Combust. Flame* **2003**, *132*, 208–218. [CrossRef]
37. Liu, H.; Liu, Y.; Yi, G.; Li, N.; Che, D. Effects of air staging conditions on the combustion and NO_x emission characteristics in a 600 MW wall fired utility boiler using lean coal. *Energ. Fuel.* **2013**, *27*, 5831–5840. [CrossRef]
38. Brown, T.D.; Smith, D.N.; O'Dowd, W.J.; Hargis Jr, R.A. Control of mercury emissions from coal-fired power plants: A preliminary cost assessment and the next steps for accurately assessing control costs. *Fuel Process. Technol.* **2000**, *65*, 311–341. [CrossRef]
39. Zhang, H.; Wang, M.; Wu, H.; Yang, H. Numerical simulation on mercury emission and transformation of occurrence state in a 410 t/h coal-fired boiler. *Proc. CSEE* **2012**, *32*, 65–70.
40. Kellie, S.; Cao, Y.; Duan, Y.; Li, L.; Chu, P.; Mehta, A.; Carty, R.; Riley, J.T.; Pan, W.-P. Factors affecting mercury speciation in a 100 MW coal-fired boiler with low-NO_x burners. *Energy Fuels* **2005**, *19*, 800–806. [CrossRef]
41. Zhuang, Y.; Thompson, J.S.; Zygarlicke, C.J.; Pavlish, J.H. Impact of calcium chloride addition on mercury transformations and control in coal flue gas. *Fuel* **2007**, *86*, 2351–2359. [CrossRef]